DETECTION OF A RELATIVISTIC IRON LINE IN MXB 1728–34 WITH
XMM-NEWTON

E. Egron[1], T. Di Salvo[2], L. Burderi[1], A. Papitto[1], L. Barragán[3], T. Dauser[3], J. Wilms[3], A. D'Aì[2], A. Riggio[1], R. Iaria[2] and N. R. Robba[2]

Abstract. We analyzed an *XMM-Newton* observation of the low-mass X-ray binary and atoll source MXB 1728–34. The source was in a low-luminosity state during the *XMM-Newton* observation, corresponding to a bolometric X-ray luminosity of $5 \times 10^{36} \ d_{5.1 \ \mathrm{kpc}}^2 \ \mathrm{erg \ s^{-1}}$. The 1–11 keV X-ray spectrum of the source, obtained combining data from all the five instruments on-board *XMM-Newton*, is well fitted by a Comptonized continuum. Evident residuals are present at $6 - 7$ keV, which are ascribed to the presence of a broad iron emission line. This feature can be equally well fitted by a relativistically smeared line or by a self-consistent, relativistically smeared reflection model. Under the hypothesis that the iron line is produced by reflection from the inner accretion disk, we can infer important information on the physical parameters of the system, such as the inner disk radius, $R_{\mathrm{in}} = 25 - 100$ km, and the inclination of the system, $44° < i < 60°$.

Keywords: line: formation, line: identification, stars: neutron, stars: individual: MXB 1728–34, X-ray: binaries, X-ray: general

1 Introduction

Broad iron emission lines in the energy range $6.4-6.97$ keV have been detected in high-energy resolution spectra of many X-ray sources containing a compact object, such as active galactic nuclei (e.g., Tanaka et al. 1995; Fabian et al. 2000) and X-ray binary systems containing a stellar-mass black hole (e.g., Miller et al. 2002; Miller 2007, for a review), or a weakly-magnetized neutron star (e.g., Bhattacharyya & Strohmayer 2007; Cackett et al. 2008; Di Salvo et al. 2009; Papitto et al. 2009; Iaria et al. 2009; D'Aì et al. 2009, and references therein). Identified with fluorescent Kα transition of iron at different ionization states, these lines are generally interpreted in terms of reflection of the central hard X-ray emission on the accretion disk (Fabian et al. 1989). Under this hypothesis, these lines are made broad and asymmetric by Doppler and relativistic effects induced by the Keplerian motion in the accretion disk near the compact object. The shape of the line is therefore an almost unique proxy of the innermost accretion disk close to the compact object (see Reynolds & Nowak 2003, for a review), and, in particular, on the inner disk radius. It also indicates the inclination angle of the system and the ionization state of the reflecting matter. Other reflection components like absorption edges and the Compton hump, which are usually observed between $20-40$ keV, are also expected to result from photoelectric absorption and Compton scattering of the main Comptonization continuum on the accretion disk matter.

MXB 1728–34 (4U 1728−34, GX 354−0) is a low-mass X-ray binary containing a weakly magnetized accreting neutron star. The optical counterpart of this "galactic bulge" source has not been identified yet, owing to the high optical extinction toward the Galactic center. Discovered in 1976 with the Small Astronomy Satellite SAS-3 (Lewin et al. 1976; Hoffman et al. 1976), this source belongs to the so-called atoll class (Hasinger & van der Klis 1989) and shows frequent type-I X-ray bursts (e.g., Basinska et al. 1984) that are caused by thermonuclear flashes on the neutron star surface.

[1] Dipartimento di Fisica, Università degli Studi di Cagliari, SP Monserrato-Sestu, KM 0.7, Monserrato, 09042 Italy

[2] Dipartimento di Scienze Fisiche ed Astronomiche, Università di Palermo, via Archirafi 36, Palermo, 90123, Italy

[3] Dr. Karl Remeis-Sternwarte and Erlangen Centre for Astroparticle Physics, Friedrich-Alexander-Universität Erlangen-Nürnberg, Sternwartstrae 7, 96049 Bamberg, Germany

Spectral analysis of MXB 1728–34 has been performed in the past using data from different satellites, such as *Einstein* (Grindlay & Hertz 1981), *SAS-3* (Basinska et al. 1984), *EXOSAT* (White et al. 1986), *SIGMA* (Claret et al. 1994), *ROSAT* (Schulz 1999), and more recently using *BeppoSAX* (Piraino et al. 2000; Di Salvo et al. 2000), *ASCA* (Narita et al. 2001), *RXTE*, *Chandra* (D'Aì et al. 2006), *INTEGRAL* (Falanga et al. 2006), and *XMM-Newton* (Ng et al. 2010).

A broad emission line at 6.7 keV has been often detected in the X-ray spectra of this source and has been interpreted as emission from highly ionized iron (e.g., Di Salvo et al. 2000). The large width of the line suggests that it could come from an ionized inner accretion disk (Piraino et al. 2000), or alternatively it could be emitted from a strongly ionized corona. D'Aì et al. (2006) have proposed an alternative model to describe the iron line region using two absorption edges associated with ionized iron instead of a Gaussian line.

We present a spectral analysis of high-energy resolution data taken by *XMM-Newton* on 2002 October 3 using all five X-ray instruments on-board this satellite. The EPIC-pn data have already been published by Ng et al. (2010), in a 'catalog' paper dedicated to the study of the iron line in 16 neutron star LMXBs observed by *XMM-Newton*. Here we present a different approach to the analysis of these data, because we fitted for the first time the *XMM-Newton* data of MXB 1728-34 with a self-consistent modeling of the continuum emission and of the reflection component. We also tried several models to fit the iron line profile, such as diskline or relline, which are different from the models proposed by Ng et al. (2010) (Gaussian or Laor). All our results favor the relativistic nature of the line profile. We simultaneously fitted the spectra from all five X-ray instruments on-board *XMM-Newton*, while the pn data alone are analyzed by Ng et al. (2010). For more detailed informations about this work, see Egron et al. (2011).

2   Observation and data reduction

MXB 1728–34 was observed by *XMM-Newton* on 2002 October 3 for a total on-source observing time of 28 ks. The $1.5 - 12$ keV lightcurve of the All Sky Monitor (ASM) on-board *RXTE* extracted within ~ 450 days the *XMM-Newton* observation indicates that the source was not in a high activity state, because it shows an average count rate of about 3 counts/s.

The *XMM-Newton* data were processed using the Science Analysis Software v. 9. The EPIC-pn camera was operated in timing mode to prevent photon pile-up. We created a calibrated photon event file using the pn processing tool EPPROC. We used the task EPFAST to correct rate-dependent CTI effects in the event list. The source spectrum was extracted from a rectangular area, covering all pixels in the Y direction, and centered on the brightest RAWX column (RAWX=38), with a width of 13 pixels around the source position . We selected only events with PATTERN ≤ 4 (single and double pixel events) and FLAG=0 as a standard procedure to eliminate spurious events. We extracted the background away from the source (in the RAWX $= 6 - 18$). We also checked that pile-up did not affect the pn spectrum using the task EPATPLOT. The total count rate registered by EPIC-pn CCDs was around 110 count/s, and was 64 count/s in the $2.4-11$ keV range, slightly increasing (by 5%) during the observation.

The MOS data were also taken in timing mode and processed with the routine EMPROC to produce calibrated event list files. The source spectra were extracted from a rectangular box centered on RAWX=320 (MOS1), and on RAWX=308 (MOS2), selecting an area 30 pixels wide around the source position, and covering 722 pixels on the Y (PHA) direction. Only events corresponding to PATTERN ≤ 12 and FLAG= 0 were selected, corresponding to standard filters. The background spectra were extracted far from the source, centered on the column RAWX= 240. We checked that the MOS spectra were not affected by pile-up. The count rates were estimated to be around 30 counts/s for each MOS unit (20 counts/s considering $2.4-11$ keV energy range).

Spectral channels of EPIC-pn and MOS spectra were rebinned to have three channels per energy resolution element and at least 25 counts per energy channel.

The two RGS were operated in the standard spectroscopy mode. The RGS data were processed using the RGSPROC pipeline to produce calibrated event list files, spectra and response matrices. The count rates measured by RGS1 and RGS2 were around 2.5 and 3.5 counts/s, respectively. The RGS data were rebinned to provide a minimum of 25 counts per energy channel.

3   Spectral analysis

Data were fitted by using XSPEC (Arnaud 1996) v.12.5.1. All uncertainties are given at the 90% confidence level ($\Delta\chi^2 = 2.706$). We simultaneously fitted the broad band energy spectra of the source obtained from all five

instruments. Considering the best calibration ranges of the different detectors, the data analysis from EPIC-pn, MOS1 and MOS2 cameras was restricted to the energy range $2.4-11$ keV. This excluded the region around the detector Si K-edge (1.8 keV) and the mirror Au M-edge (2.3 keV) that could affect our analysis. We only used the RGS1 and RGS2 data between $1-2$ keV to constrain the softest band.

The different cross calibrations of the five instruments were taken into account by including normalizing factors in the model. These factors were fixed to 1 for pn and kept free for the other instruments.

We first fitted the continuum with a thermal Comptonized model using COMPTT (Titarchuk 1994), modified at low energy by the interstellar photoelectric absorption modeled by PHABS. The χ^2/degrees of freedom (d.o.f.) of the fit was large, 1732/903. We then tried to add a blackbody component (BBODY model) to improve the fit. The addition of this component turned out not to be statistically significant, thus we decided not to include the blackbody in our model.

With respect to this continuum model, an excess was present in the residuals between 5.5 and 8 keV, probably indicating the presence of iron discrete features. The fit was improved by adding a broad iron emission line, modeled by a simple Gaussian line (Model 1), centered at 6.6 keV with the σ parameter frozen at 0.6 keV. With the addition of the Gaussian, the fit gave a χ^2/d.o.f. $= 1489/901$ (resulting in a significant improvement of the fit, with a $\Delta\chi^2 = 243$ for the addition of two parameters).

We then tried to substitute the Gaussian at 6.6 keV with a diskline profile and obtained a slightly better result with a χ^2/d.o.f. $= 1463/899$. Owing to the large uncertainties on the outer radius of the disk and on the inclination of the system if they were let free, we froze the first one at 1000 R_g and the inclination at 60° (the source does not show any dip in its lightcurve, implying $i < 60°$). The improvement of the fit corresponds to $\Delta\chi^2 = 26$ for the addition of two parameters (the F-test gives a probability of chance improvement of about 10^{-4}).

To assess the significance of the relativistic line smearing on a statistical basis, we used another statistical method based on the posterior predictive p values described by Hurkett et al. (2008). For simplicity, we restricted our data to two instruments (pn and MOS2). These data were fitted with Model 1 and Model 2, respectively. We obtained an improvement of the fit corresponding to a $\Delta\chi^2$ of 18 for the addition of two parameters when we substituted Model 1 with Model 2. Then, we simulated 200 pn and MOS2 spectra according to Model 1, which were fitted in a second step using Model 2. The $\Delta\chi^2$ was registered for each simulation. Among the 200 simulations, we twice found a $\Delta\chi^2$ higher than 18. So the probability of chance improvement we gain from these simulations is 1%, which agrees with the 0.75% calculated by the F-test performed on the real data restricted to two instruments. Therefore, we can conclude that the diskline model is to be preferred because it gives a probability of chance improvement of the fit of about 10^{-4} using all instruments.

This model gives an estimate of the inner radius of the disk $R_{in} \sim 18$ R_g ($R_g = GM/c^2$ is the gravitational radius). Fixing the inclination to lower values (i.e. $i < 60°$), worse χ^2 were obtained with the other diskline parameters drifting toward lower R_{in}, higher rest-frame energies, and higher emissivity indices in absolute value. We searched for an absorption edge in the energy range $7-10$ keV, but none was significantly detected.

To fit the iron line, we also used a new model for a relativistically distorted diskline, called RELLINE* (Dauser et al. 2010), which calculates line profiles taking into account all relativistic distortions in a disk around the compact object. We also fixed the outer radius of the disk and the inclination of the system to the same values used in the diskline model. The χ^2/d.o.f. obtained in these conditions is 1464/899. The best-fit line parameters obtained in this way are perfectly consistent with those obtained using the diskline model. In particular this model (Model 3) estimates the inner radius of the disk to be $R_{in} \sim 19$ R_g.

We tried an alternative model for the iron features (see D'Aì et al. 2006) using two absorption edges (instead of an emission line), which are found at 7.50 keV ($\tau \sim 0.06$) and 8.49 keV ($\tau \sim 0.06$), associated to mildly and highly ionized iron, respectively. The χ^2/d.o.f. for this fit is 1519/899 (which has to be compared to 1489/901 that we obtained fitting the iron line with a Gaussian (Model 1) or to 1463/899 that we obtained fitting the iron line with a diskline (Model 2)). Therefore this model gives a worse fit of the iron features than the previous ones.

In order to test the consistency of the broad iron line with a reflection component, we fitted the data using REFLION, a self-consistent reflection model including both the reflection continuum and the corresponding discrete features (Ross & Fabian 2005), in addition to a thermally Comptonized continuum modeled with NTH-COMP, by Zdziarski et al. (1996), and extended by Zycki et al. (1999)), instead of COMPTT. The χ^2/d.o.f. was 1555/901, without the inclusion of relativistic smearing. Because the iron line was found to be significantly

---

*‘urlhttp://www.sternwarte.uni-erlangen.de/research/relline/.

broad in the previous models (Model 1, 2, and 3), we added the relativistic smearing using the RDBLUR component. The addition of this component to the model constitutes Model 5 and led to a $\chi^2/\text{d.o.f.} = 1466/899$. The decrease of the χ^2 for the addition of the relativistic smearing was $\Delta\chi^2 = 89$ for the addition of two parameters (corresponding to an F-test probability of chance improvement of $\sim 10^{-12}$). Assuming that iron has a solar abundance and freezing the emissivity betor index to -2.8 (value obtained with the diskline model) and the ionization parameter $\xi = L_X/(nr^2)$ to 660 (this parameter tends to take high values but is unstable during the fit, which is why we preferred to freeze it), where L_X is the ionizing X-ray luminosity, n is the electron density in the reflector, and r the distance of the reflector to the emitting central source, the inner radius was estimated again to be 20 R_g and a lower limit to the inclination angle was found to be 44°. In Fig. 1 we plot the residuals obtained with this self-consistent reflection model in comparison with the continuum and the RELLINE model using the EPIC-pn data.

The residuals found with respect to the different models described above do not show any evident systematic trend; the large χ^2 could be due to mismatches in the cross-calibration between the different instruments (for more details, see the cross-calibration document available on the *XMM-Newton* webpage[†]) or to unresolved and unfitted features.
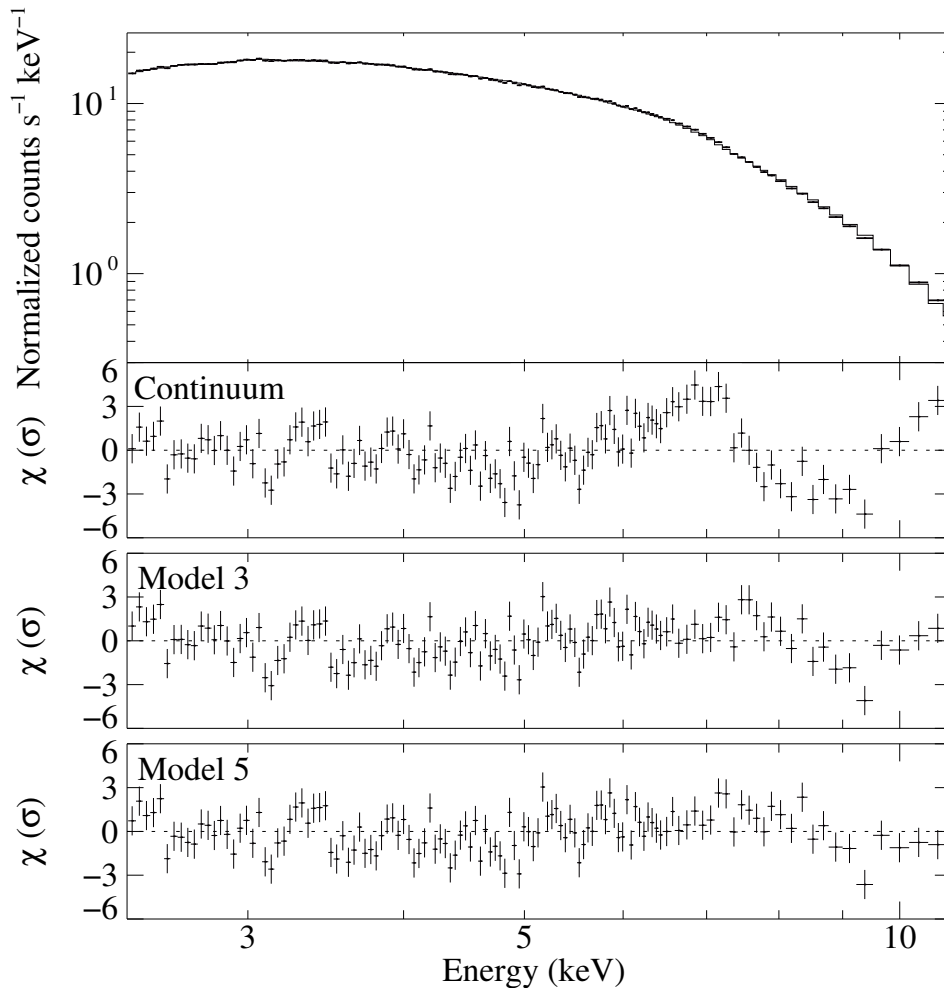
Fig. 1. Top: EPIC-pn data points of MXB 1728–34 in the range 2.4−11 keV. **Bottom**: Residuals (data-model) in unit of sigmas for the continuum, for Model 3 including a relativistic line (RELLINE), and for Model 5 using a relativistic reflection component (REFLION), respectively. Data were rebinned for graphical purposes.

[†]`http://xmm2.esac.esa.int/docs/documents/CAL-TN-0052.ps.gz`.

4 Discussion

We performed a spectral analysis of MXB 1728–34 observed by *XMM-Newton* on 2002 October 3 in the $1-11$ keV energy range. The best-fit continuum model consists of an absorbed Comptonized component; the addition of a soft blackbody component does not improve the fit significantly. With respect to this continuum model, evident residuals are present at $6-8$ keV, which can be fitted either by a relativistic line (such as diskline or RELLINE) or by a self-consistent relativistic reflection model.

4.1 The continuum emission

The X-ray spectra of black-hole and neutron star in X-ray binaries are generally described by models that include a soft/thermal and a hard/Comptonized component; the electron temperature of the Comptonized component significantly decreases when the source transits from the hard to the soft state while its optical depth increases. We chose a continuum that consists of an absorbed Comptonization model (COMPTT or NTHCOMP) because these models gave the best fit to the broad-band $(0.1-200$ keV) *BeppoSAX* spectrum of MXB 1728–34 (Piraino et al. 2000; Di Salvo et al. 2000).

Usually a soft blackbody component is required to fit the broad band X-ray spectra of LMXBs, most frequently interpreted as emitted by an accretion disk. This component is not significantly detected in the *XMM-Newton* spectrum. This may be ascribed to the relatively low X-ray luminosity of the source during the *XMM-Newton* observation, specially in the soft band. The bolometric X-ray flux in the range $0.1-150$ keV also implies a bolometric X-ray luminosity of $L_X \sim 5 \times 10^{36} d_{5.1}^2$ erg s^{-1}, corresponding to 2% of the Eddington luminosity, that is $L_{\mathrm{Edd}} = 2.5 \times 10^{38}$ erg s^{-1} for a 1.4 M$_\odot$ neutron star (e.g., van Paradijs & McClintock 1994). Indeed, during the high/soft state the disk is expected to be very close to the compact object, while in the low/hard state the disk should be truncated far from the compact object, and therefore its contribution is expected to be less important.

We conclude that the blackbody component is just too weak to be detected. This agrees with the results obtained from the fit of the iron feature with a reflection model. This indicates that the inner accretion disk is probably truncated far from the neutron star ($R_{\mathrm{in}} > 25$ km), and with a relatively high value for the system inclination with respect to the line of sight estimated at $44° < i < 60°$, which would further reduce the disk luminosity with respect to the Comptonized component in the hypothesis that the last one has a spherical geometry around the compact object.

4.2 The iron line emission

Recently Ng et al. (2010) and Cackett et al. (2010) presented a spectral analysis of a sample of neutron star LMXBs observed by *XMM-Newton* and *Suzaku,* respectively, with particular interest in the iron discrete features in these sources. While Cackett et al. (2010) conclude that Fe K line profiles are well fitted by a relativistic line model for a Schwarzschild metric in most cases and imply a narrow range of inner disk radii ($6-15\ GM/c^2$), Ng et al. (2010) conclude there is no evidence for asymmetric (relativistic) line profiles in the *XMM-Newton* data, although the line profiles (fitted with a simple Gaussian or a laor model) again appear to be quite broad, with Gaussian sigmas ranging between 0.17 up to 1.15 keV.

We tried different models to fit the iron line profile. Although a Gaussian line provides an acceptable fit of the line profile, we tried to physically interpret its large width using models for a relativistically smeared line in an accretion disk.

Using the diskline profile (Model 2), we find the line centroid energy at 6.45 keV, compatible with a fluorescent $K\alpha$ transition from mildly ionized iron Fe I–XX. The inner radius is in the range $12-21\ R_g$. The line profile appears therefore to be significantly broad and compatible with a diskline profile. The results obtained by using a relativistic line profile corresponding to Model 3, which uses the more recent RELLINE instead of diskline, are perfectly consistent with the diskline model. The inner radius is estimated to be in the range $15-22\ R_g$.

The line profile can be equally well fitted using a self-consistent relativistic reflection model (Model 5). The addition of the RDBLUR component significantly improves the χ^2. This indicates that the line is indeed broad, and that the width of the line agrees with a relativistic smearing in the disk. The value of the inner radius is again consistent with that found using a diskline or a relline profile, even if the uncertainty is larger ($R_{\mathrm{in}} = 13$-$43\ R_g$). For a neutron star mass of 1.4 M$_\odot$, the inner disk radius is in the range $25-100$ km from the neutron star center, and so the disk would be truncated quite far from the neutron star surface. The inclination angle

of the system with respect to the line of sight is found to be $> 44°$, which is still compatible with the absence of dips in its lightcurve (which implies $i < 60°$).

We therefore favor the interpretation of the iron feature as a broad and relativistic emission line produced in the accretion disk, because this gives a better fit of the *XMM-Newton* spectrum and very reasonable values of the reflection parameters.

References

Arnaud, K. A. 1996, in ASP Conf. Ser. 101: Astronomical Data Analysis Software and Systems V, 17

Basinska, E. M., Lewin, W. H. G., Sztajno, M., Cominsky, L. R., & Marshall, F. J. 1984, ApJ, 281, L337

Bhattacharyya, S. & Strohmayer, T. E. 2007, ApJ, 664, L103

Cackett, E. M., Miller, J. M., Ballantyne, D. R., et al. 2010, ApJ, 720, L205

Cackett, E. M., Miller, J. M., Bhattacharyya, S., et al. 2008, ApJ, 674, L415

Claret, A., Goldwurm, A., Cordier, B., et al. 1994, ApJ, 423, L436

D'Aì, A., Di Salvo, T., Iaria, R., et al. 2006, A&A, 448, 817

D'Aì, A., Iaria, R., Di Salvo, T., Matt, G., & Robba, N. R. 2009, ApJ, 693, L1

Dauser, T., Wilms, J., Reynolds, C. S., & Brenneman, L. W. 2010, MNRAS, 409, 1534

Di Salvo, T., D'Aì, A., Iaria, R., et al. 2009, MNRAS, 398, 2022

Di Salvo, T., Iaria, R., Burderi, L., & Robba, N. R. 2000, ApJ, 542, L1034

Egron, E., Di Salvo, T., Burderi, L., et al. 2011, A&A, 530, A99

Fabian, A. C., Iwasawa, K., Reynolds, C. S., & Young, A. J. 2000, PASP, 112, 1145

Fabian, A. C., Rees, M. J., Stella, L., & White, N. E. 1989, MNRAS, 729

Falanga, M., Gotz, D., Goldoni, P., et al. 2006, A&A, 458, 21

Grindlay, J. E. & Hertz, P. 1981, ApJ, 247, L17

Hasinger, G. & van der Klis, M. 1989, A&A, 225, 79

Hoffman, J. A., Lewin, W. H. G., Doty, J., et al. 1976, ApJ, 210, L13

Hurkett, C. P., Vaughan, S., Osborne, J. P., et al. 2008, ApJ, 679, L587

Iaria, R.and D'Aì, A., di Salvo, T., Robba, N. R., et al. 2009, A&A, 505, 1143

Lewin, W. H. G., Clark, G., & Doty, J. 1976, iauc, 2922, 1

Miller, J. M. 2007, ARA&A, 45, 441

Miller, J. M., Fabian, A. C., Wijnands, R., et al. 2002, ApJ, 570, L69

Narita, T., Grindlay, J. E., & Barret, D. 2001, ApJ, 547, L420

Ng, C., Diaz Trigo, M., Cadolle Bel, M., & Migliari, S. 2010, A&A, 522, A96

Papitto, A., Di Salvo, T., D'Aì, A., et al. 2009, A&A, 493, 39

Piraino, S., Santangelo, A., & Kaaret, P. 2000, A&A, 360, 35

Reynolds, C. S. & Nowak, M. A. 2003, Phys. Rep., 377, 389

Ross, R. R. & Fabian, A. C. 2005, MNRAS, 358, 211

Schulz, N. S. 1999, ApJ, 511, L304

Tanaka, Y., Nandra, K., Fabian, A. C., et al. 1995, Nature, 375, 659

Titarchuk, L. 1994, ApJ, 434, L570

van Paradijs, J. & McClintock, J. E. 1994, A&A, 290, 133

White, N. E., Peacock, A., Hasinger, G., et al. 1986, MNRAS, 218, 129

Zdziarski, A. A., Johnson, W. N., & Magdziarz, P. 1996, MNRAS, 283, 193

Zycki, P. T., Done, C., & Smith, D. A. 1999, MNRAS, 309, 561